Effects of the two-color laser on relativistic muon motion[*]

SHI Chun-Hua (石春花),[1, †] SU Jin (苏晋),[2] and ZHOU Jin-Yang (周晋阳)[1]

[1]*Department of Biomedical Engineering, Changzhi Medical College, Changzhi 046000, China*
[2]*Department of Physics, Changzhi Medical College, Changzhi 046000, China*

Considering the mixture after muon-catalyzed fusion (μCF) reaction as overdense plasma, we analyze muon motion in the plasma induced by a linearly polarized two-colour laser, particularly, the effect of laser parameters on the muon momentum and trajectory. The results show that muon drift along the propagation of laser and oscillation perpendicular to the propagation remain after the end of the laser pulse. Under appropriate parameters, muon can go from the skin layer into field-free matter in a time period of much less than the pulse duration. The electric-field strength ratio or frequency ratio of the fundamental to the harmonic has more influence on muon oscillation. The laser affects little on other particles in the plasma. Hence, in theory, this work can avoid muon sticking to α effectively and reduce muon-loss probability in μCF.

I. INTRODUCTION

The muon catalyzed fusion (μCF) of hydrogen isotopes, especially D-T fusion, has been studied as a realizable candidate of an energy source as thermal energies [1–7]. In the liquid mixture of D_2 and T_2, the muon plays the role of a catalyzer through the formation of a muonic molecule. After the fusion process, the muon is released normally and again it is utilized for a subsequent fusion until the muon decays. However, in fact, after the μCF, some muon may be strapped by α particles and form into $(\alpha\mu)^+$. This has become a major limitation on the number of fusion cycles catalyzed by each muon [8, 9]. Because of muon-loss, μCF is far from the aim to attain energy plus. In the past decade, researchers found sticking phenomena and new insights in μCF [10–14], and in experiments μCF numbers per muon extend to 150 during the lifetime of $\sim 2.2 \times 10^{-6}$ s [15]. Althought this catalyzed efficiency is not enough for atomic energy application, muon regeneration from the α-sticking has been increasingly studied.

In this work, we were trying to avoid muon-α sticking by inducting an external force. Here, the laser is a good choice. It is well-known that ultra-short, ultra-intense laser pulses are potentially useful for a variety of applications. Recently, ultra-short lasers have been applied extensively to studies of electron acceleration schemes due to their potential of offering compact and low-cost setups through accelerator gradients several orders of magnitude higher than those of conventional RF linear accelerators [16–18]. Unlike one-color laser, a two-color laser beam is the sum of two copropagating pulsed radially polarized laser beams, with central angular frequencies ω and $n\omega$, of unequal pulse duration and peak power. Also, the relative phase of the two-color laser pulses

adds one more degree of freedom [19]. Previous simulations have shown that a one-color pulsed radially polarized laser beam can accelerate an initially stationary electron only up to 40% of the theoretical energy gain limit [20, 21], while a two-color pulsed beam can accelerate an electron by over 90% of the one-color beam's theoretical gain limit, for a given total energy and pulse duration [22]. So, in order to make the muon well out of the mixture, the choice of the two-color laser becomes especially important [23, 24].

In this paper, the two-color laser is induced in the D-D fusion, and muon can be moved at a certain track so that μ is not captured by α. To study the muon drift of D-D fusion in the two-color laser, it is necessary to choose some appropriate laser parameters. Here, we explore the possibility of the muon drift and trajectory, particularly; study influences of various laser-pulse parameters (i.e., frequency, intensity, and relative phase) on the muon drift and investigate coherent effects on other particles in a two-level field.

II. COMPUTATIONAL MODEL AND METHOD

When a cycle of μCF(d-d): $\mu + d + d \rightarrow dd\mu \rightarrow \alpha + n + \mu$ is just finished, the α and μ particles are existing independently, i.e. the μ ions are not captured by the α particles. Then, at the moment, there is the mixture which consists of α, neutron (n), electron (e), d, and μ in the fusion reaction target. It is known that the use of a plasma medium is an attractive way of achieving laser-driven electron acceleration [17]. So, we consider the above mixture as the plasma with a frequency ω_p, ($\omega_p^2 = \omega_{p\alpha}^2 + \omega_{pe}^2 + \omega_{p\mu}^2$, $\omega_{p\alpha}$, ω_{pe} and $\omega_{p\mu}$ are frequency of α, e and μ, respectively). Also, as $\omega_{pe} \gg \omega_{p\mu} \gg \omega_{p\alpha}$, we judge $\omega_p^2 = \omega_{pe}^2$.

At the same time of the above mixture formation, the two-color laser pulse is turned on and off adiabatically, i.e.

$$E(t) = f(t) \cdot \{E_f \exp(-i\omega_f t) + E_h \exp[-i(\omega_h t + \varphi)]\}, \quad (1)$$

where, subscript f denotes the fundamental part in the two-color laser pulse and subscript h denotes the harmonic part;

E_f and E_h are amplitude of the electric-field strength of the fundamental laser field and the harmonic field, respectively; for the frequency ω_f and ω_h, the nth harmonic field means $\omega_h = n\omega_f$; φ is the relative phase between the fundamental field and the harmonic; and $f(t)$ is the shape of the laser pulse, i.e.

$$f(t) = \sec h^2(t/\tau), \qquad (2)$$

where, τ is the pulse duration. When the plasma frequency ω_p meets the relation of $\omega_p \gg \omega_h > \omega$ ($\omega = (\omega_f + \omega_h)/2$ is the equivalent frequency of a two-color laser), the laser beam can be considered propagating in overdense plasma [25].

For the sake of simplicity, we assume that the linearly polarized laser beam propagates perpendicular to the plane surface of the target. Let us direct the axis X along the propagation of the laser pulse, the axis Y along the electric-field strength, and the axis Z along the magnetic-field strength. Throughout the paper, the system of units $m_e = e = c = 1$ is used. A laser beam propagates in overdense plasma with a plasma frequency ω_p greater than the laser frequency ω in the skin layer having a depth $\delta = 1/\omega_p$. The boundary conditions for the electric and magnetic fields on the surface vacuum-overdense plasma are of the well-known form:

$$
\begin{aligned}
F^{\text{in}} &= \frac{2}{1+\sqrt{\varepsilon}} F(\text{t}) \approx \frac{2}{\sqrt{\varepsilon}} F(\text{t}), \\
B^{\text{in}} &= \frac{2\sqrt{\varepsilon}}{1+\sqrt{\varepsilon}} F(\text{t}) \approx 2F(\text{t}),
\end{aligned}
\qquad (3)
$$

where, F^{in} is the electric-field amplitude inside the plasma, $F(t)$ meets the relation of $F(\text{t}) = |E(t)|$ and $varepsilon$ is the dielectric constant of plasma, i.e. $\varepsilon = 1 - \omega_p^2/\omega^2 \approx -\omega_p^2/\omega^2$.

Then, the Newton classical equations for muon momentum P_x and P_y inside the skin layer ($x > 0$) are of the form:

$$
\begin{cases}
k\dfrac{\mathrm{d}P_x}{\mathrm{d}t} = 2\nu_y f(t)\exp(-x/\delta)\{E_f \sin(\omega_f t) \\
\qquad\qquad + E_h \sin(\omega_h t + \varphi)\} \\
k\dfrac{\mathrm{d}P_y}{\mathrm{d}t} = 2\dfrac{\omega}{\omega_p} f(t)\exp(-x/\delta)\{E_f \cos(\omega_f t) \\
\qquad\qquad + E_h \cos(\omega_h t + \varphi)\} \\
\qquad\qquad - 2\nu_x f(t)\exp(-x/\delta)\{E_f \sin(\omega_f t) \\
\qquad\qquad + E_h \sin(\omega_h t + \varphi)\}
\end{cases}
\qquad (4)
$$

where $k = m_\mu/m_e \approx 207$, $\delta = 1/\omega_p$ is the depth of the skin layer, and $x = 0$ is the surface of the target. The velocity ν_x and ν_y are given by

$$
\begin{aligned}
\nu_x &= \frac{\mathrm{d}x}{\mathrm{d}t} = \frac{P_x}{\sqrt{1^2 + P_x^2 + P_y^2}}; \\
\nu_y &= \frac{\mathrm{d}y}{\mathrm{d}t} = \frac{P_y}{\sqrt{1^2 + P_x^2 + P_y^2}}.
\end{aligned}
\qquad (5)
$$

III. NUMERICAL RESULTS AND ANALYSIS

We assume that there is no muon motion along the magnetic-field strength, i.e. the axis Z. Besides, collisions of muons are neglected in our consideration. Eqs. (4) and (5) can be solved with the initial conditions that at the time instance $t = -\infty$ a muon is at rest when $x = y = 0$. Of course, the average muon velocity along the Y axis is zero. After the end of a laser pulse, a muon has zero velocity in the Y direction and nonzero velocity in the X direction.

A. The effect of electric-field strength

The relativistic plasma frequency is $\omega_p = (4\pi n_e/\gamma)^{1/2}$, $\gamma = [1 + (F^{\text{in}}/\omega)^2]^{1/2}$ is the relativistic factor. From Eq. (1) to Eq. (5), we fixed the value $\omega_p/\omega_f = 21/2$ and $\omega_f\tau/\pi = 40$ in our numerical computation which correspond to the pulse duration $\tau = 83\,\text{fs}$ and the electron number density $n_e = 8 \times 10^{22}\,\text{cm}^{-3}$. For the two-color laser, we take the 2th harmonic field $\omega_h = 2\omega_f$ and the relative phase $\varphi = 0$. Based on the above values, by solving the Eqs. (4) and (5), the muon motion is determined only by one dimensionless parameter $g = 4E_f/(3\omega_f)$ and the amplitude ratio of the electric-field strength E_f/E_h. The value $g = 1$ corresponds to the peak laser intensity of $5 \times 10^{17}\,\text{W/cm}^2$ (at the laser photon energy $\hbar\omega = 1.5\,\text{eV}$).
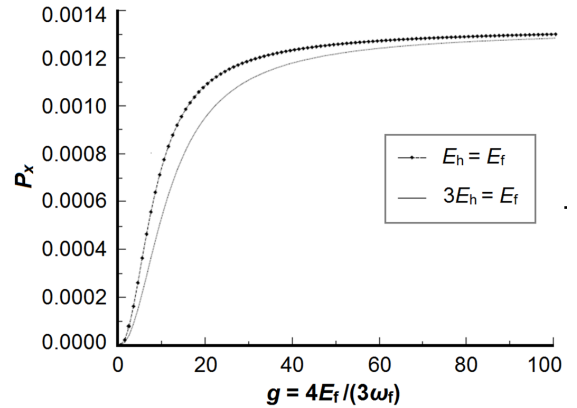

Fig. 1. The dependences of the muon momentum P_x on the dimensionless parameter g.

Figure 1 shows the dependence of muon momentum P_x (in units of $m_e c$, in this paper, the units of the momentum are all $m_e c$.) on the value of g and the different ratio of E_f to E_h, where we take $E_h = E_f$ and $3E_h = E_f$, respectively. The value g from 0 to 100 corresponds to the peak laser intensity of $0 \sim 5 \times 10^{21}\,\text{W/cm}^2$. The results show that the two curves change in a similar way basically. The momentum increases with the laser intensity, but it is a nonrelativistic quantity ($P_x \ll m_e c$) even at the relativistic peak laser intensity $5 \times 10^{21}\,\text{W/cm}^2$. Fig. 1 also shows the different ratio of the fundamental electric-field strength to the harmonic has effects on the muon momentum P_x, but the effect is obvious
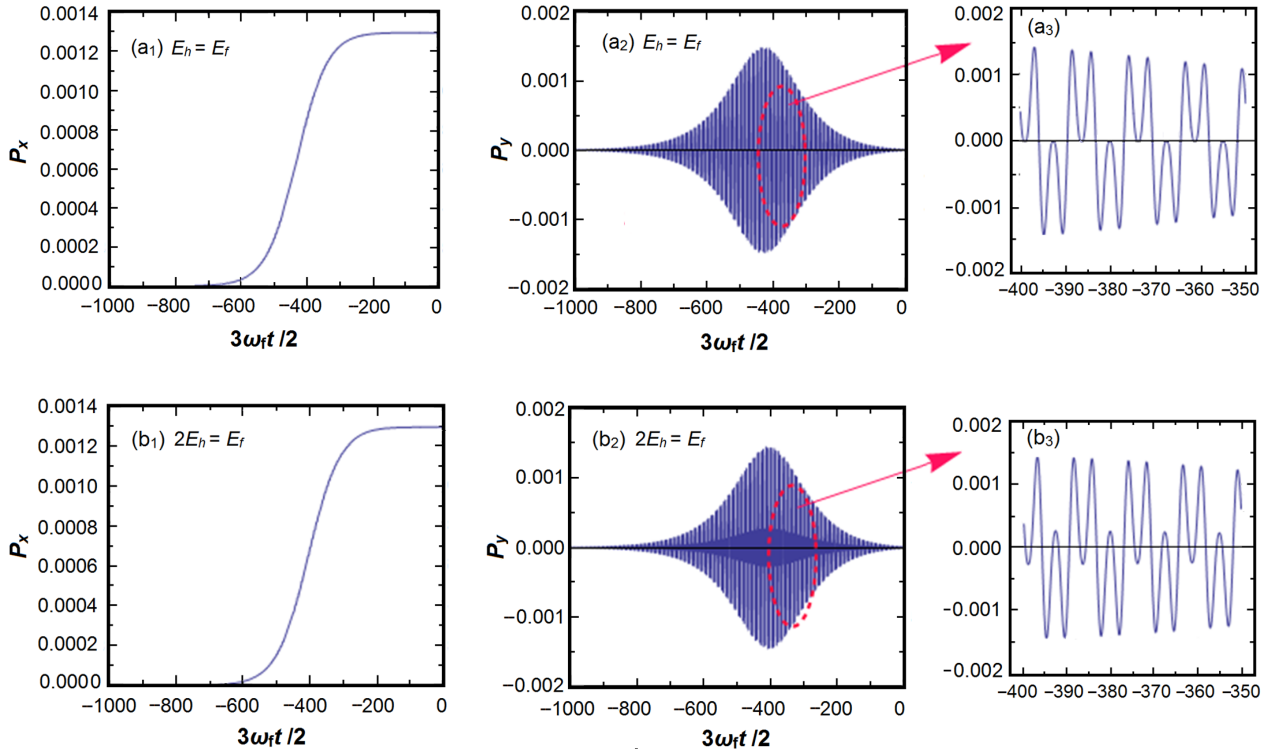
Fig. 2. (Color online) The muon momentum P_x and P_y change for the value of the dimensionless parameter $g = 80$.

at $g = 0 \sim 70$ and is not obvious at $g > 70$.

Figure 2 demonstrates the muon momentum P_x and P_y at the leading edge of the laser pulse for the typical value of $g = 80$ (the peak laser intensity of the fundamental wave is 3.2×10^{21} W/cm^2 according to Eqs. (4) and (5), with $E_h = E_f$ in Fig. 2(a$_1$–a$_3$) and $2E_h = E_f$ in Fig. 2(b$_1$–b$_3$). As can be seen in the figures, a muon goes from the skin layer inside field-free matter before the laser pulse ($\propto \sec h^2(t/\tau)$) reaches its maximum because of the small depth of the skin layer. i.e. a muon stops acceleration on the rear border of the skin layer. It is also obvious that $P_y \rightarrow 0$ when a muon leaves the skin layer, because of adiabaticity of the laser pulse. In addition, the different E_f/E_h ratio affects little on the muon momentum in the X axis, but obviously in the Y axis (Figs. 2(a$_3$) and 2(b$_3$)).

The muon trajectory in the plane for $g = 80$ is shown in Fig. 3. The dimensionless muon coordinates x and y are given in units of the skin depth δ. The amplitude of muon oscillations in the transverse direction Y is much less than its drift motion in the direction of laser pulse propagation (the X axis). This indicates that a muon penetrates many skin depths into field-free matter even before the laser pulse reaches its maximum. The amplitude and shape of muon oscillations in the transverse direction Y in Figs. 3(a) and 3(b) differ from each other, due to different harmonic wave electric-field strength. At a greater $m = E_f/E_h$, the amplitude of muon oscillations in the transverse direction Y reduces and the shape is more complicated.

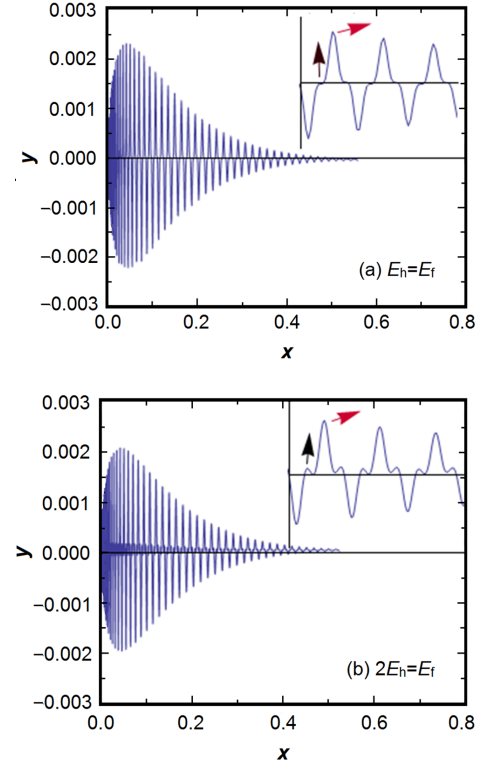To explain that a muon goes from the skin layer inside

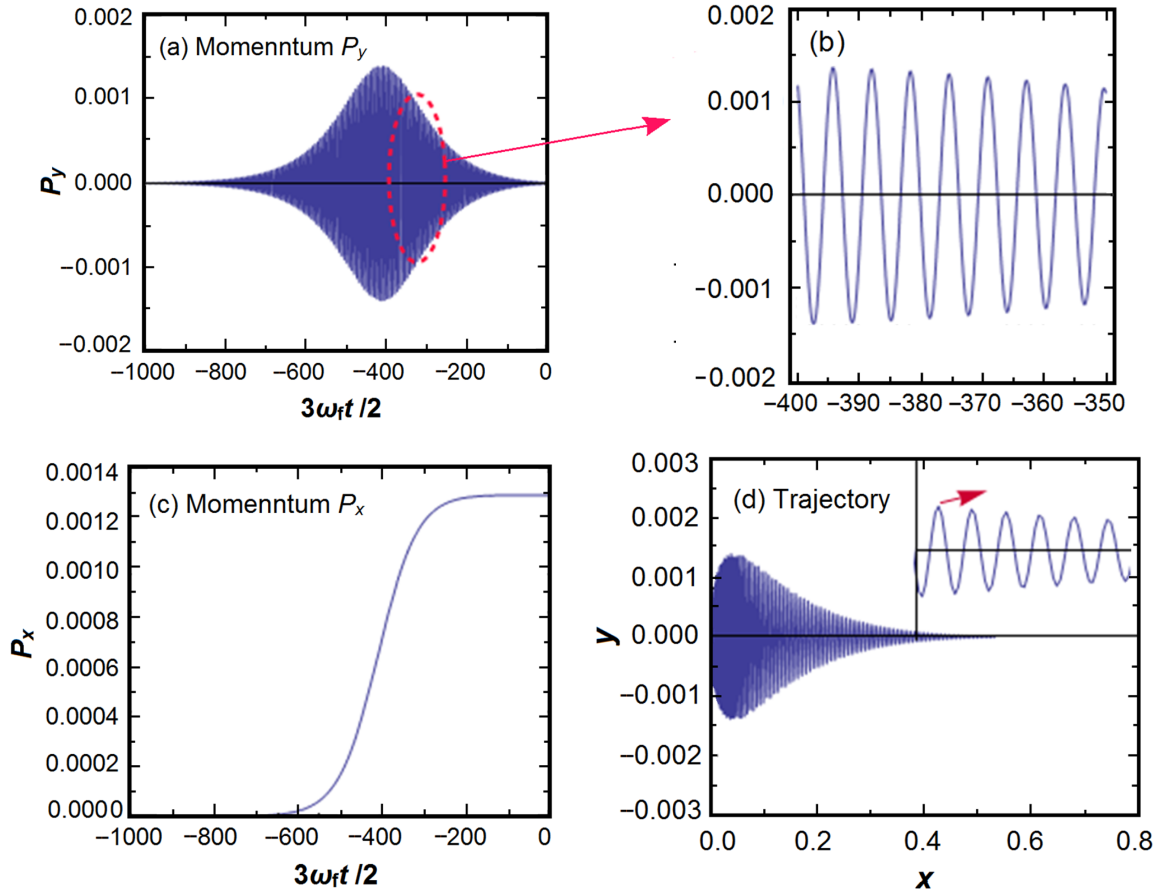Fig. 3. (Color online) The muon trajectory.

Fig. 4. (Color online) The muon motion in one-color laser field.

field-free matter or penetrates many skin depths into field-free matter before the laser pulse reaches its maximum, we make an estimate qualitatively. We consider that the muon drift velocity in the direction of laser pulse propagation has the estimate $\nu_x = N(E_f/\omega_p)^2$ from Eq. (4). Then, the time t_p for penetration of the skin layer having the depth δ is approximately, i.e. $t_p = \delta/\nu_x = \omega_p/(NE_f^2) \approx 48\,\text{fs}$. The result shows $t_p < \tau$, i.e. the time t_p at which a muon goes into field-free matter from the skin layer is much less than the laser duration τ. Thus, a muon goes quickly from the skin layer into field-free matter.

Besides, in order to better illustrate effects of the two-color laser intensity on muon motion, we calculate the muon momentum and trajectory in one-color laser (Fig. 4, in a peak laser intensity of 6.4×10^{21} W/cm^2 and other parameters being the same value as the above. In Fig. 4(c) the maximum of muon momentum P_x in the one-color laser field is less than in Fig. 2(a$_1$). It shows that the influence of the two-color laser intensity on the momentum is not a simple addition of two one-color laser beams, and a two-color pulsed beam can accelerate muon to the same maximum with lower intensity. In Figs. 4(a) and 4(b), the oscillations of muon momentum P_y in the one-color laser field are different from Fig. 2(a$_2$) and 2(a$_3$). The muon oscillations have just one peak in ev-

ery cycle in one-color laser field (Fig. 4(b)) but two peaks in two-color laser field (Fig. 2(a$_3$)). The muon trajectory in the one-color laser field is shown in Fig. 4(d), where the amplitude of muon oscillations in the transverse direction Y is obviously less than that in the two-color laser field (Fig. 3(a)). In Fig. 3(a), the muon oscillation in each cycle has two peaks (red and black arrows) in the two-color laser field, but in Fig. 4(d) it has a single peak (red arrow). Certainly, in the one-color laser field, a muon goes from the skin layer inside field-free matter before the laser pulse reaches its maximum, and $P_y \to 0$ when a muon leaves the skin layer. However, a muon takes a longer time to go into field-free matter from the skin layer in the one-color field than in the two-color field.

B.   The effect of frequency

To evaluate the frequency effect, we still fix the pulse duration $\tau = 83\,\text{fs}$ and the electron density $n_e = 8 \times 10^{22}$ cm^{-3}. For the two-color laser, we take $2E_h = E_f$, $E_f = 8.0 \times 10^{20}$ W/cm^2 and $\varphi = 0$. Therefore, the muon motion is determined only by the dimensionless parameter ω_p/ω ($\omega = (\omega_f + \omega_h)/2$) and the frequency ratio of the fundamental laser field ω_f to the harmonic field ω_h.
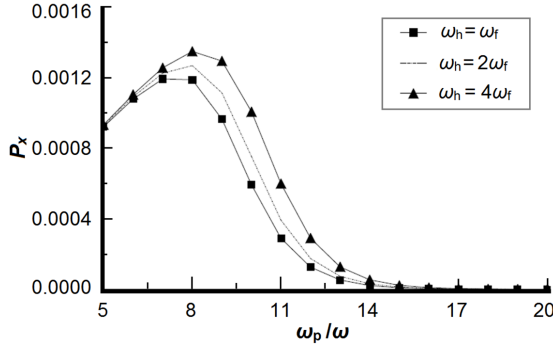
Fig. 5. The dependences of the muon momentum P_x on the dimensionless parameter of ω_p/ω.

Figure 5 shows the dependence of muon momentum P_x on ω_p/ω, and on ω_f/ω_h, at $\omega_h = \omega_f$, $\omega_h = 2\omega_f$ and $\omega_h = 4\omega_f$, respectively. The ω_p/ω changes from 5 to 20 so that the plasma frequency ω_p is far larger than the laser frequency ω. In Fig. 5, the three curves change in a similar way basically, but different frequency ratio affects the muon momentum P_x, especially at $\omega_p/\omega = 6 \sim 14$. Besides, the three curves have different peak positions.

Figure 6 shows the muon momentum P_x and P_y at the leading edge of the laser pulse for typical value of the peak laser intensity of the fundamental wave being 8.0×10^{20} W/cm^2 and $\omega_p/\omega = 8$ according to Fig. 5. We take $\omega_h = 2\omega_f$ in Figs. 6(a$_1$) and 6(a$_2$) and $\omega_h = 4\omega_f$ in Figs. 6(b$_1$) and 6(b$_2$). From the figures, a muon goes from the skin layer inside field-free matter before the laser pulse reaches its maximum, and $P_y \to 0$ when a muon leaves the skin layer. In addition, the frequency ratio affects the muon momentum obviously in the X axis and the Y axis. At a higher frequency ratio, i.e. a greater $n = \omega_h/\omega_f$, the maximum of the muon momentum P_x increase, and so does the amplitude of the muon oscillations of P_y in the Y axis, with a more complicated shape.

Figure 7 shows the muon trajectory in the plane for the peak laser intensity of fundamental wave 8.0×10^{20} W/cm^2 and $\omega_p/\omega = 8$. The dimensionless muon coordinates x and y are given in units of the skin depth δ. The amplitude of muon oscillations in the transverse direction Y is much less than its drift motion in the direction of laser pulse propagation (the X axis). This indicates that a muon penetrates the skin depths into field-free matter even before the laser pulse reaches its maximum. At a greater $n = \omega_h/\omega_f$, with an increased muon momentum in the X and the Y axises, the amplitude of muon oscillations in the transverse direction Y increases while the frequency of muon oscillations reduces. Thus, the muon oscillations in the Y axis reduce and at the same time the muon leaves the skin layer by a faster speed in the X axis.

In the same way, based on above parameters, the time t_p at which a muon goes into field-free matter from the skin layer is about 44 fs. A smaller-than-τ t_p means that a muon penetrates the skin depth into field-free matter before the laser pulse reaches its maximum. So, the muon leaves the skin layer faster to enter the free field, at $\omega_p/\omega = 8$ and peak laser intensity of $E_f = 8.0 \times 10^{20}$ W/cm^2, than the results in

Sec. III. A at much larger parameters of g and E_f.

C.   The effect of relative phase

For the two-color laser with the parameters of $\omega_p/\omega = 8$, $E_f = 8.0 \times 10^{20}$ W/cm^2, electron number density $n_e = 8.0 \times 10^{22}$ cm^{-3}, $2E_h = E_f$ and $\omega_h = 2\omega_f$, the muon motion is determined only by the pulse duration τ and the relative phase φ. The relative phase in two-color lasers means the propagation distance in the plasma media. It can be converted into the media length $L = \varphi\lambda_h/(2\pi)$.

Figure 8 shows the muon momentum P_x at the relative phase of $\varphi = \pi/6$ ($L = \lambda_h/12$) and the pulse duration $\tau = 10 \sim 100$ fs. At $\tau < 50$ fs, the muon momentum P_x is less than those in Sec. III. A and Sec. III. B, hence a longer t_p, the time for penetrating the skin layer of the depth δ. Then, probably, once the laser pulse duration is less than 50 fs, the muon cannot penetrate the skin layer at the end of a pulse. Thus, to study the effect of the relative phase on the muon trajectory, we take $\tau = 50$ fs.

Figure 9 shows the muon momentum P_y at the leading edge of the laser pulse, with peak laser intensity of the fundamental wave being 8.0×10^{20} W/cm^2 at $\omega_p/\omega = 8$, $\tau = 50$ fs, and the relative phase $\varphi = 0$ ($L = 0$), $\pi/4$ ($L = \lambda_h/8$), $\pi/2$ ($L = \lambda_h/4$) and $3\pi/4$ ($L = 3\lambda_h/8$). We also find that the relative phase φ has obvious effects on the muon momentum in just the Y axis. The muon oscillations shape and the peak change with the relative phase. The red and the black arrows indicate peaks that change constantly with the relative phase. Because the relative phase has less effect on the muon momentum P_x, the muon trajectories are similar to the results above. The muon speed in the X axis is not affected and the muon still can penetrate skin depths into field-free matter. However, as shown in Fig. 10, in the transverse direction Y, the muon oscillations are in different amplitudes and shapes at different relative phases. In Figs. 9 and 10, at greater the relative phases, the muon oscillation peaks marked with red arrows increase while the muon oscillation peaks marked with black arrows reduce consistently.

D.   The effects of muon initial velocity

For all above analysis, initial velocity of muon is neglected in our consideration, i.e. Eqs. (4) and (5) can be solved with the initial conditions that $\nu(t = -\infty) = 0$. In fact, after every μCF reaction, velocity of muon is not zero but its value is not unique. Most muons are free, and their velocity depends on the energy release of nuclear fusion [13]. Some muons stick to alpha particles and form muonic helium ions, and the initial sticking probability is 0.912% [26]. Where muonic helium ions are formed with energy of 3.47 MeV, they are slowed down toward thermal energy by collision with the surrounding D$_2$ and DT molecules [27]. So, muonic helium ions can be stripped as a result of collisions and some muons regain free, probability of which is 25% [28]. Their velocities are much less. Other muonic helium ions may be stripped by the
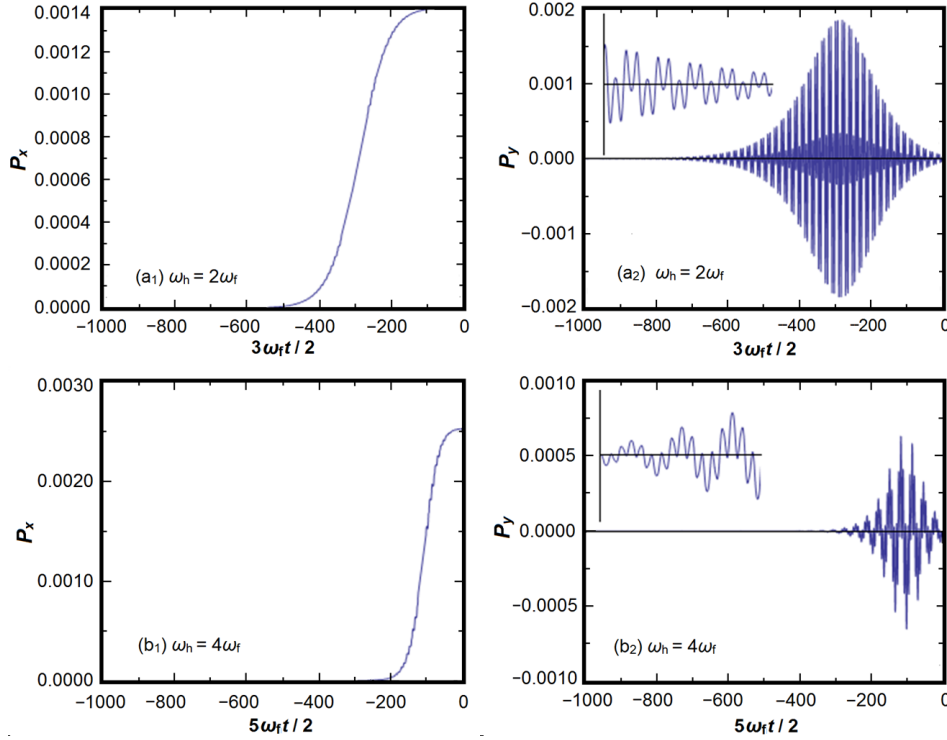
Fig. 6. (Color online) The muon momentum P_x and P_y change for the value of the dimensionless parameter $\omega_p/\omega = 8$.
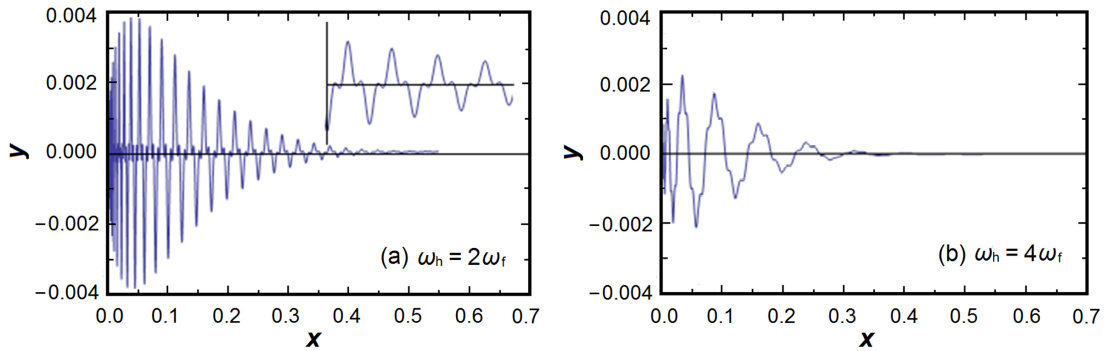

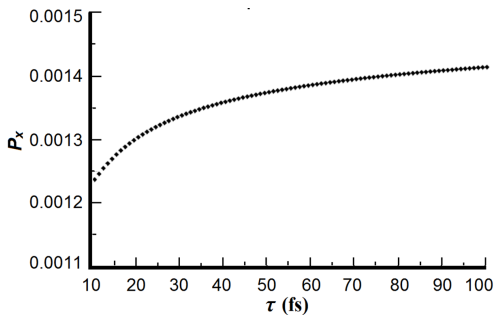
Fig. 7. (Color online) The muon trajectory.

Fig. 8. The dependences of muon momentum P_x on the pulse duration τ at the relative phase of $\varphi = \pi/6$.

external force [29] and velocity of free muon are related to the force. Based on the energy release of nuclear fusion, we take two value of initial velocity and solve the Eqs. (4) and (5).

Figure 11 shows the muon momentum P_x and P_y at the leading edge of the laser pulse and where values of relevant parameters are the same with Fig. 2(a$_1$−a$_3$). The only different is the value of muon initial velocity. According to Eqs. (4) and (5), we take the initial velocity $\nu_x = \nu_y = 0.001$ in Fig. 11(a$_1$−a$_3$), and $\nu_x = \nu_y = 0.0001$ in Fig. 11(b$_1$−b$_3$), instead of $\nu_x = \nu_y = 0$ in Fig. 2(a$_1$−a$_3$), the unit of velocity is $c = 3 \times 10^8$ m/s. The results shows that a muon goes from the skin layer inside field-free matter before the laser pulse reaches its maximum, and $P_y \to 0$ when a muon leaves the skin layer. Comparing Figs. 11(a$_3$) and 11(b$_3$), the detail changes of P_y, the muon initial velocity has obvious effect on
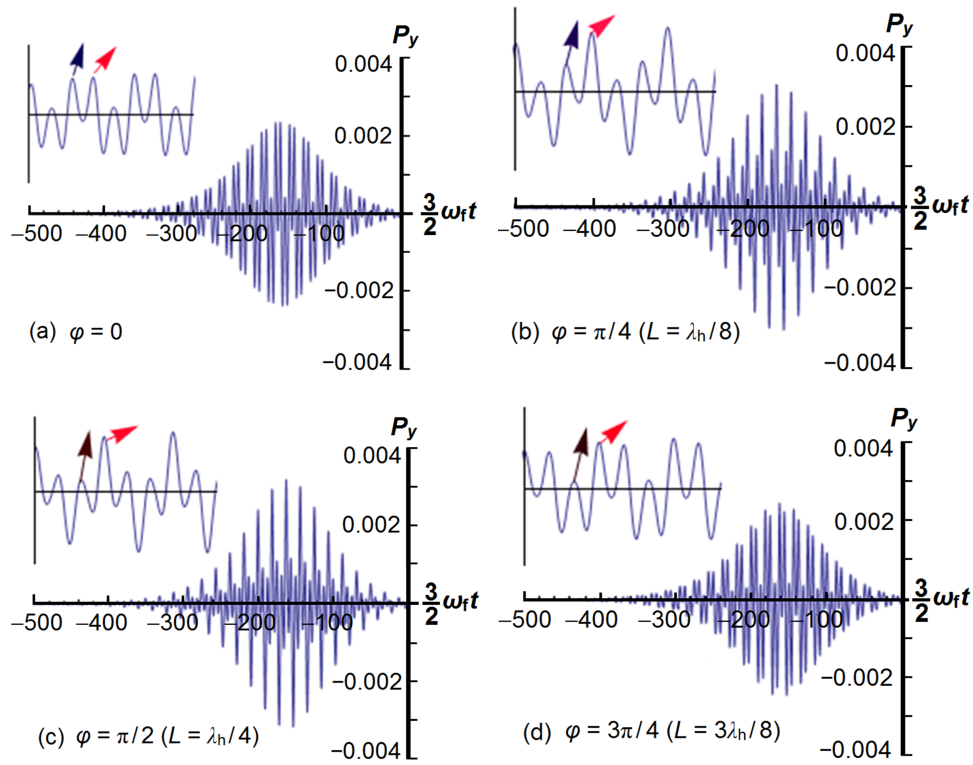
Fig. 9. (Color online) The muon momentum P_y change for the pulse duration $\tau = 50\,\text{fs}$.
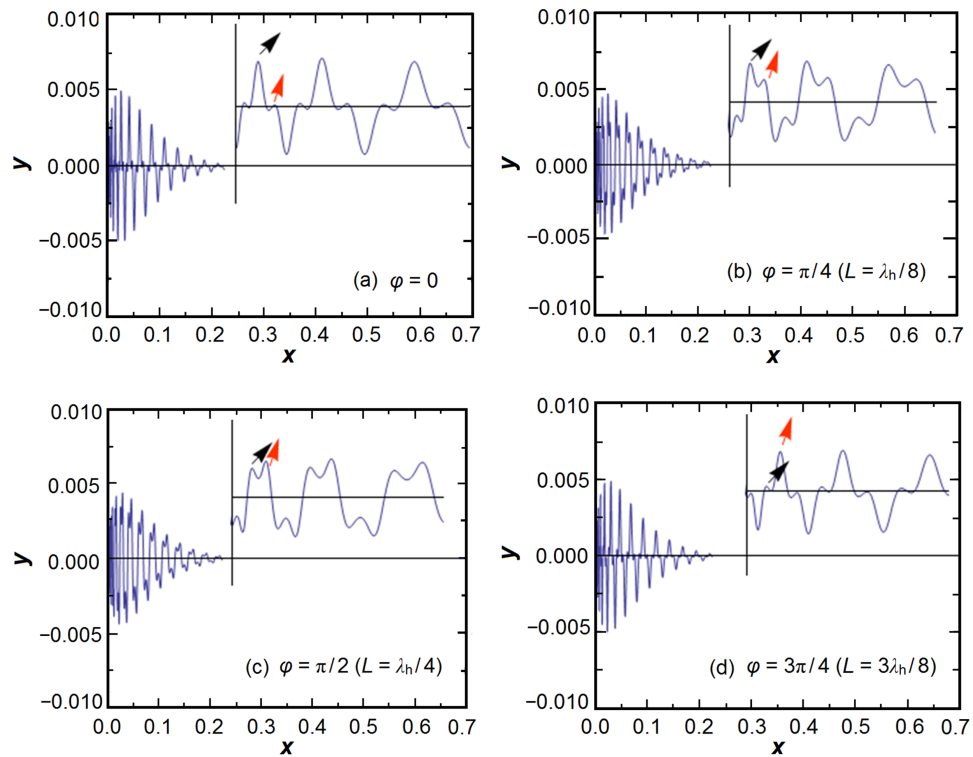

Fig. 10. (Color online) The muon trajectory.

the muon momentum in the Y axis, while it has a little effect on the muon momentum in the X axis. In the case of super-
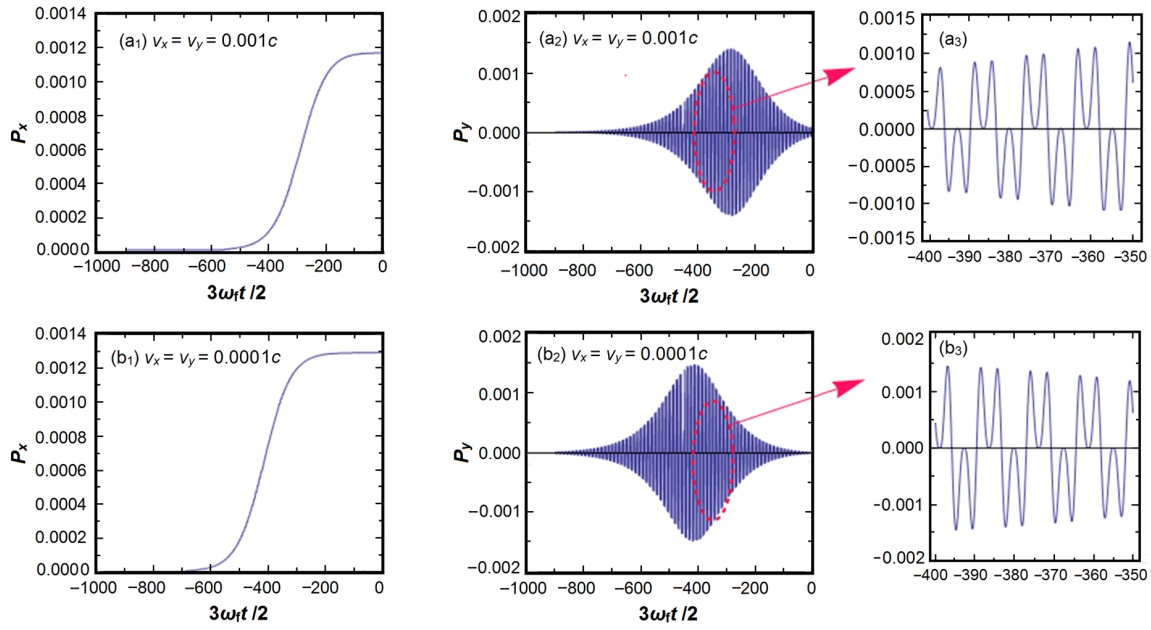
Fig. 11. The muon momentum P_x and P_y at $g = 80$ in muon initial velocity of $0.001c$ and $0.0001c$ ($c = 3 \times 10^8$ m/s).

intense laser pulses, the initial velocity in the X axis plays a little role in muon drift, for muon has relatively high drift velocities induced by the laser in the X axis.

IV. DISCUSSION AND CONCLUSION

In addition, with the induction of the two-color laser, we have to consider the influence of the laser on other particles in the overdense plasma. According to similar methods, we study the other particles trajectory in different muzzle velocities. Because the muzzle velocity of other particles is small, the laser has little influence on them, i.e. the motion of those particles produced by the superintense laser pulse is far less than the motion of muons. Also, the duration of laser pulse is so short that the work does not introduce the disadvantage into μCF reaction in the superintense laser, but make the muon penetrate skin depths into field-free matter to avoid the

α-sticking.

In this paper, we consider the mixture after μCF (d-d) reaction as overdense plasma with the frequency ω_p, and the two-color lasers with the frequency ω_h and ω_f are induced. We study the effect of two-color laser parameters on the muon momentum and trajectory, including the peak intensity, ratio of the fundamental electric-field strength to the harmonic, frequency ratio, relative phase and pulse duration. We find that the time at which a muon penetrates into field-free matter from the skin layer is much less than the pulse duration τ under the right conditions. This penetration occurs at the leading edge of the laser pulse. The muon drift in overdense plasma along the propagation of laser radiation produced by a magnetic part of a laser field remains after the end of the laser pulse. Hence, after μCF (d-d) reaction is finished and before the muon is captured by α, inducting a suitable superintense laser pulse can avoid the α-sticking efficiently.

[1] Gershtein S S, Petrov I V, Ponomarev L I, *et al*. Zh Eksp Teor Fiz+, 1980, **78**: 2099–2111.

[2] Alexander S A, Froelich P, Monkhorst H J. Phys Rev A, 1990, **41**: 2854–2857.

[3] Ponomarev L I. Contemp Phys, 1990, **31**: 219–245.

[4] Petitjean C, Atchison F, Heidenreich G, *et al*. Fusion Technol, 1994, **25**: 437–449.

[5] Nagamine K, Matsuzaki T, Ishida K, *et al*. Hyperfine Interact, 1999, **119**: 273–280.

[6] Nakamura S N, Nagamine K, Matsuzaki T, *et al*. Phys Lett B, 2000, **473**: 226–232.

[7] Nagamine K. Nucl Energy, 2005, **3B**: 555–602.

[8] Ceperley D and Alder B J. Phys Rev A, 1985, **31**: 1999–2004.

[9] Davies J D, England J B A, Pyle G J, *et al*. J Phys G Nucl Partic, 1990, **10**: 1529–1537.

[10] Ishida K, Okamoto K, Kawasaki Y, *et al*. Phys Rev Lett, 2002, **89**: 107202.

[11] Nagamine K and Ponomarev L. Nucl Phys A, 2003, **721**: c863–c866.

[12] Ishida K, Nagamine K, Matsuzaki T. Nucl Phys B, 2005, **149**: 348–350.

[13] Kimura S and Bonasera A. Radiat Eff Defect S, 2008, **163**: 287–292.

[14] Balin D V, Ganzha V A, Kozlov S M, *et al*. Phys Part Nuclei, 2011, **42**: 185–214.

[15] He J T. Physics, 2003, **18**: 461–466.(in Chinese)

[16] Malka V, Faure J, Gauduel Y A, *et al*. Nat Phys, 2008, **4**: 447–453.

[17] Esarey E, Schroeder C B, Leemans W P. Rev Mod Phys, 2009, **81**: 1229–1285.

[18] Salamin Y I, Hu S X, Hatsagortsyan K Z, *et al*. Phys Rep, 2006, **427**: 41–155.

[19] Shi C H, Qiu X J, Li R X. J Mod Optic, 2007, **54**: 1435–1444.

[20] Wong L J and Kärtner F X, Opt Express, 2010, **18**: 25035.

[21] Fortin P L, Piché M, Varin C. J Phys B, 2010, **43**: 025401.

[22] Liang J W and Franz X K. Opt Lett, 2011, **36**: 957–959.

[23] Zhao K and Chu T S. Chem Phys Lett, 2011, **511**: 166–171.

[24] Johnson L A, Palastro J P, Antonsen T M, *et al*. Phys Rev A, 2013, **88**: 063804.

[25] Rastunkov V S and Krainov V P. Phys Rev E, 2004, **69**: 037402.

[26] Hu C Y, Hale G M, Cohen J S. Phys Rev A, 1994, **49**: 4481–4488.

[27] Jones S E. Nature, 1986, **321**: 127–133.

[28] Zeldovich Y B and Gershtein S S. Sov Phys Uspekhi, 1961, **3**: 593–623.

[29] Shi C H, Qiu X J, An W K, *et al*. Acta Phys Sin, 2005, **54**: 4087–4091.(in Chinese)